Microstructure of Room Temperature Ionic Liquids at Stepped Graphite Electrodes

Guang Feng, Song Li, and Wei Zhao
State Key Laboratory of Coal Combustion, School of Energy and Power Engineering, Huazhong University of Science and Technology, Wuhan 430074, China

Peter T. Cummings
Dept. of Chemical and Biomolecular Engineering, Vanderbilt University, Nashville, TN 37235, USA

DOI 10.1002/aic.14927
Published online July 14, 2015 in Wiley Online Library (wileyonlinelibrary.com)

Molecular dynamics simulations of room temperature ionic liquid (RTIL) [emim][TFSI] at stepped graphite electrodes were performed to investigate the influence of the thickness of the electrode surface step on the microstructure of interfacial RTILs. A strong correlation was observed between the interfacial RTIL structure and the step thickness in electrode surface as well as the ion size. Specifically, when the step thickness is commensurate with ion size, the interfacial layering of cation/anion is more evident; whereas, the layering tends to be less defined when the step thickness is close to the half of ion size. Furthermore, two-dimensional microstructure of ion layers exhibits different patterns and alignments of counterion/co-ion lattice at neutral and charged electrodes. As the cation/anion layering could impose considerable effects on ion diffusion, the detailed information of interfacial RTILs at stepped graphite presented here would help to understand the molecular mechanism of RTIL-electrode interfaces in supercapacitors. © 2015 American Institute of Chemical Engineers *AIChE J*, 61: 3022–3028, 2015

Keywords: electrical double layer, interfacial microstructure, room temperature ionic liquids, graphite electrode, energy storage

Introduction

The use of electricity generated from renewable but intermittent energy sources (e.g., solar and wind energy) requires high-efficient energy storage equipment. Supercapacitor, also called electrical double layer capacitor (EDLC), is an advanced green energy storage device due to its advantageous properties, such as high power density, long cycle life, quick charge and discharge processing, wide operating temperature, and environmental friendliness.[1–5] However, the industrialization and the impact of supercapacitors in current energy storage community cannot be comparable to batteries worldwide, as the moderate energy density of supercapacitors limits their wider applications.[6] Thus, the current supercapacitor development aims at increasing its energy density.[4]

According to the theoretical formula of supercapacitor's energy density (E): $E = A \cdot C \cdot V^2/2$, the energy density can be increased via[7,8] (1) developing the electrode with high specific surface area (A); (2) choosing an appropriate electrode/electrolyte assemble to increase the specific capacitance (C); (3) widening operating voltage (V) of supercapacitors. With high specific surface area, good thermal and electrical conductivity, and electrochemical stability,[9] carbons, such as graphite and carbon nanotubes, have been one of the most considerable electrode materials in supercapacitors. Ionic liquids (ILs) are emerging as a new type of green electrolytes developed in recent decades. They entirely consist of ions and stay in liquid state at or near room temperature with outstanding features, such as high thermal stability, low volatility, high conductivity, noninflammability, nonoxidability, nonexplosion, and so on.[10–12] In particular, with the wider electrochemical window compared with solvent-containing electrolytes (e.g., aqueous solution: 1.2 V, organic solvent solution: 2.7 V), ILs render a high operating voltage (4–6 V)[13] which helps to improve the energy density of supercapacitors. Therefore, the use of graphene-based electrode and IL electrolytes in supercapacitors could enhance the energy density, opening up a new possibility for environment-friendly and high-performance supercapacitors.

A myriad of experimental and theoretical studies using IL electrolytes in supercapacitors have been reported,[4,5,14–18] most of which focus on the solid-liquid interfacial phenomenon. Mezger et al.[19] observed a hierarchical structure of staggeredly distributed cations and anions in double layers formed by ILs near the charged solid surface with the help of high-energy X-ray diffraction technique. Atkin et al.[20–23] have reported a series of experiments on the microstructure of confined ILs at different surfaces using atomic force microscope (AFM) and scanning electron microscopy (SEM). The microstructure of imidazolium-/pyrrolidinium-based ILs between two negatively charged mica surfaces was analyzed by Perkin et al.,[24–28] in which three different physical models were

Correspondence concerning this article should be addressed to G. Feng at gfeng@hust.edu.cn.

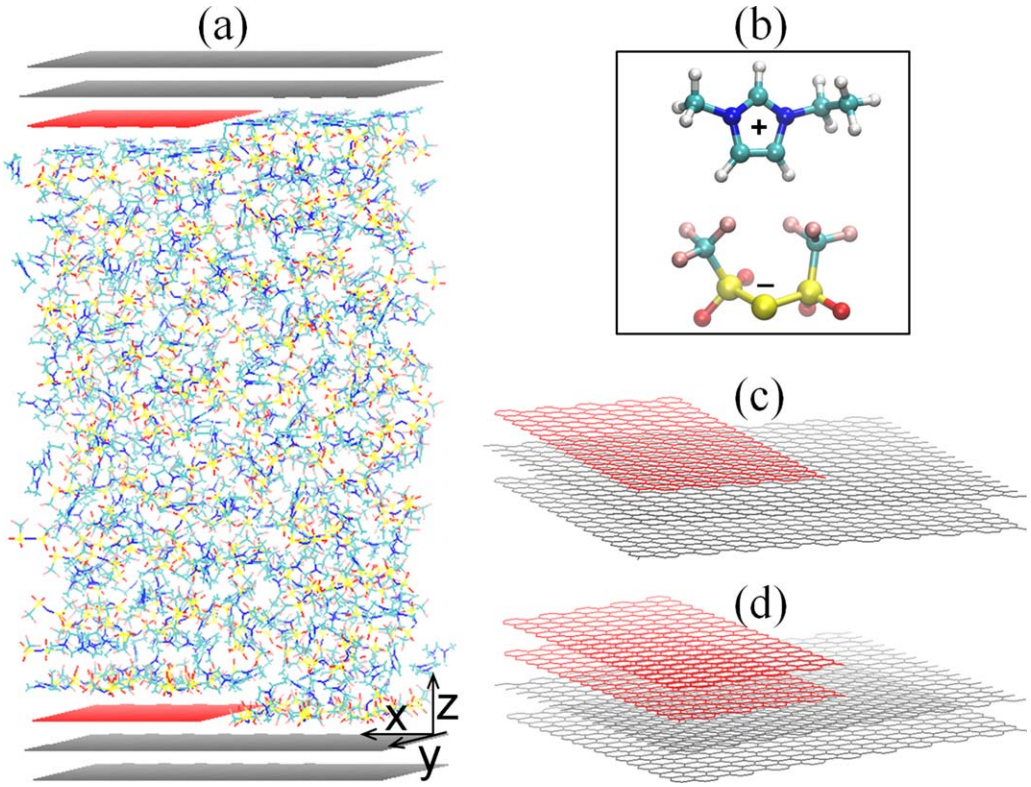

Figure 1. (a) Typical simulation cell for ILs/electrode system, (b) molecular structures of the cation and anions in [emim][TFSI], (c) the graphite electrode with one stepped structure (1-step), and (d) the graphite electrode with two stepped structure (2-step).

[Color figure can be viewed in the online issue, which is available at wileyonlinelibrary.com.]

proposed to describe the microstructure of different ILs in charged slit pores. Similarly, theoretical studies, especially by molecular dynamics (MD) simulation, have revealed the microscopic structure of ILs-electrode interfaces in atomistic scale.[18,29–31] Through MD simulation of imidazolium-based ILs represented by an all-atom model, Wang[32] and Vatamanu et al.[30] observed a similar staggered hierarchical structure in EDL at planar graphite electrode surface. That is, the EDL can be extended to 1.5–3.0 nm from the electrode and the ILs beyond this region are distributed randomly; in addition, imidazolium ring at interface was found to be parallelized with electrode surface, regardless of the alkyl chain length. It is worthwhile to note that the ratio of theoretical studies to experimental works on ILs-electrode interfaces is ~1:50,[33] indicating a crucial need of more theoretical work in this area. In our recent work,[34] MD simulations were used to analyze the distribution of ILs at the planar carbon surface and provided a good fit to experimental data from AFM measurements. It also suggests that AFM tips can penetrate the first ion adsorption layer and probe the layering of ions at atomistic scale.

However, most of the simulation studies (including ours) adopted the ideally planar electrode, while the real electrode mostly has defects that make it challenging to accurately characterize the ILs-electrode interface. The microstructure of ILs at an uneven electrode surface is not only critical for understanding the energy storage mechanism of EDL at supercapacitor electrodes, but also significant for elucidating the behavior of IL lubricants at liquid-solid interfaces.[35] In this work, MD simulations were performed to reveal the microstructure of ILs at stepped electrode surface. We mainly investigated the effect of step thickness on interfacial IL structure and illuminated the mechanism underlying the impact of stepped graphene surface on ILs distribution.

Methods

As shown in Figure 1a, the microscopic interface formed by ILs at different topological graphene surfaces is represented by a channel-like model in this work. IL 1-ethyl-3-methylimidazolium bis(trifluoromethylsulfonyl)imide ([emim][TFSI], Figure 1b) is chosen as the electrolyte between two electrodes. Each electrode contains two complete graphene monolayers and one or two half monolayers (Figures 1c, d); the distance between each two layers is 0.341 nm. To easily quantify the ion distribution at interface, the first complete layer that directly contacts ILs is set as zero in z direction (Figure 1a); the stepped electrodes are labeled as 1-step (Figure 1c) and 2-step (Figure 1d) according to the number of half graphene monolayer(s) involved. The size of graphite electrodes in xy plane is 4.26 nm × 4.18 nm; the distance between two electrodes is fixed at ~8.0 nm, which ensures the ILs in the middle of the channel in bulk state. To investigate the interfacial phenomenon in supercapacitors after applying a potential, small partial charges were placed on a planar image surface that is 0.07 nm away from the inner graphene sheet directly contacting with ILs, which could mimic the potential applied on electrodes.[36] The charge densities (σ) of the electrode surface are 0.0 and 0.1 C/m^2 in this work; for the charged electrodes, to neutralize the overall MD system, the lower and upper electrodes in Figure 1a carry charges with the same amount but an opposite sign. Meanwhile, the

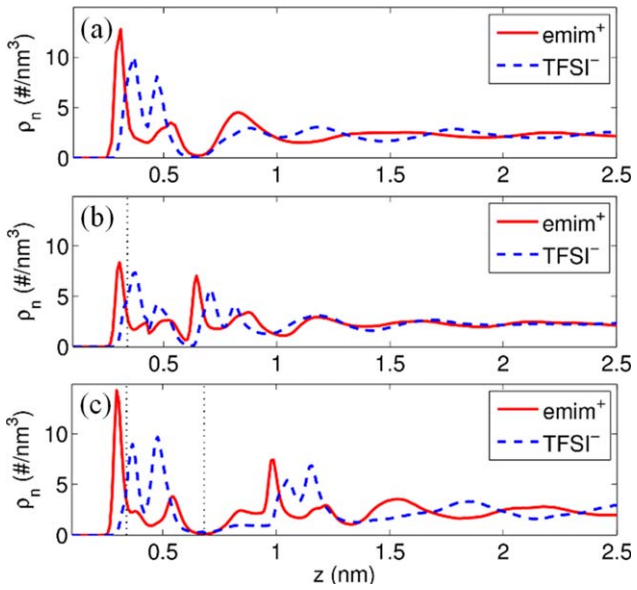

Figure 2. Density distribution profiles of ions at neutral electrode surface.

(a) Planar electrode (0-step electrode), (b) 1-step electrode (see Figure 1c), and (c) 2-step electrode (see Figure 1d). The vertical dashed lines are used to show the position of stepped graphene. [Color figure can be viewed in the online issue, which is available at wileyonlinelibrary.com.]

simulation of electrodes without steps (denoted as 0-step) is also performed to comparatively analyze the effect of stepped surface structure on ILs. The number of ion pairs between two electrodes was tuned to make the IL density in the middle of the channel very similar (within 1.2%) to that in a bulk simulation. Furthermore, additional simulations were performed to evaluate the dependence of IL-electrode interfacial structures on the IL density at the channel center, by reducing the channel-central IL density by 4.1% compared with bulk density. It is found that the IL-electrode interfacial structures are insensitive to the precise value of the IL density at the channel center. The force fields for the electrode atoms (carbon) and ILs were obtained from Ref. 37.

Simulations were carried out in the NVT ensembles using a user-modified version of MD package GROMACS.[38] In the simulation system, the electrolyte temperature was maintained at 298 K using the Nose–Hoover thermostat. The slab-PME method[39] was used to compute the electrostatic interactions in the two-dimensionally periodic geometry adopted here. Specifically, the dimension vertical to electrode of the simulation box was set to be five times the electrode separation,[40] which is sufficient to ensure that the accuracy of electrostatic force calculation is comparable to that of the two-dimensional (2-D) Ewald method.[39] An FFT grid spacing of 0.10 nm and cubic interpolation for charge distribution were used to compute the electrostatic interactions in reciprocal space. The cutoffs for both Coulombic and van der Waals interactions are 1.1 nm. LINCS algorithm[41] is used to constrain all chemical bonds of ions. The simulation was initially run for 1 ns at a very high temperature (1000 K) to accelerate the movement of ions for a quite random initial configuration; then, the system was annealed gradually to 298 K within 3 ns; finally, the system was equilibrated at constant temperature (298 K) for another 6 ns, and then a 12-ns production was performed for data analysis.

Results and Discussions

The effect of step thickness on the microstructure of ILs at stepped graphite electrode surface was first investigated by analyzing the number density (ρ_n) profiles of cation ($emim^+$) and anion ($TFSI^-$) near neutral electrodes. Note that the mass center of an ion is used for the number densities of all ions in this work); from the easier to the more advanced, in this section, one-dimensional (1-D) microscopic structures were first discussed, followed by the 2-D structure analysis. As shown in Figure 2, it is observed that there is a cation peak accompanying with an anion peak located at 0.25–0.55 nm from electrode because of the ion-electrode interactions and cation-anion coupling; cations and anions have a hierarchical structure of staggered distribution with oscillatory behaviors, similar to previous work.[18,29,30]

However, in contrast to nonstepped planar electrodes, remarkable phenomena in stepped structure were observed: (1) there is an extra outstanding cation-anion coupling layer in stepped graphite except the one closest to the intact graphene surface (Figures 2b, c); (2) the ILs near 1-step electrode exhibit the lowest oscillation amplitude (Figure 2b) while the 2-step structure shows the highest (Figure 2c). The first phenomenon may be attributed to the joint effect of the cation/anion layers formed at the exposed intact graphene and those formed at the exposed half-sized graphene, leading to the enhanced ion density at the second peak. However, such explanation seems contradictory with the observation in phenomenon 2 that shows different ion layering. Recent work indicated that different distributions of ions could impose a great effect on charge/discharge process in supercapacitors, due to the strong correlation between diffusion/microscopic

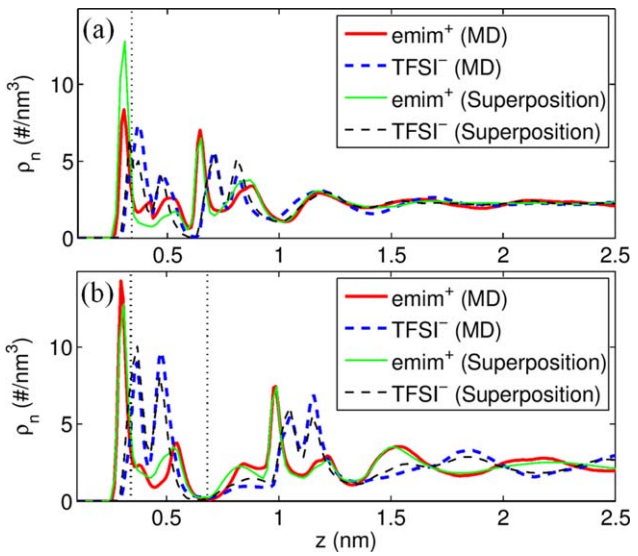

Figure 3. The comparison between density distributions of ions at planar electrode surface after superposition and in MD simulation with stepped electrode surface.

(a) 1-Step electrode; (b) 2-step electrode. In legend, MD indicates that the ion distributions are generated from stepped electrode simulation system, and superposition represents that it is a theoretical density distribution based on interference theory. The dashed lines perpendicular to the z axis show the position of stepped structure. [Color figure can be viewed in the online issue, which is available at wileyonlinelibrary.com.]

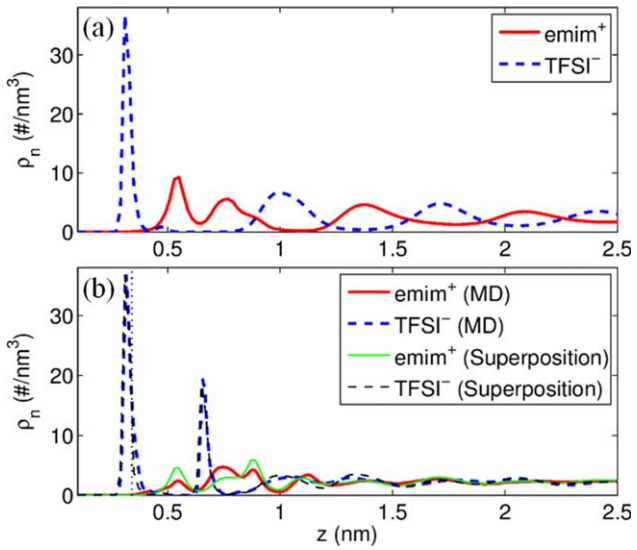

Figure 4. When the charge density of electrode is 0.1 C/m^2, (a) the microstructure of EDL at 0-step electrode surface, (b) the comparison between ion distribution functions at 1-step electrode surface before and after superposition.

[Color figure can be viewed in the online issue, which is available at wileyonlinelibrary.com.]

flow of ions and ion distribution (e.g., counterion/co-ion lattice pattern).[42]

To reveal the mechanism underlying the second phenomenon, EDL interference theory,[43,44] similar to the wave interference in physics, is used: the EDL structure contains both peak and trough, similar to the wave; when two EDLs interfere with each other, the high cation/anion peaks will form an enhanced peak at the location where they meet, while the low ones will form an declined peak. According to this concept of EDL interference, the interfered ion distribution at stepped electrode surface (Figure 3) was derived by the superposition of ion distribution functions at an ideal graphite surface (Figure 2a). Specifically, the ion distribution function, $\rho_n(z)$, in Figure 2a is shifted toward the channel center by one or two layer spacing, L, (0.341 nm or 0.682 nm) of graphene along z direction (Figure 1a), and then superimposed with the unshifted one to obtain the ion distribution as a result of interference. The ion distribution via such an interference would be expressed mathematically as $\rho_{tot}(z) = \rho_n(z)$ when $z \leq L$ and $\rho_{tot}(z) = [\rho_n(z) + \rho_n(L + z)]/2$ when $z > L$.

According to Figure 3, the superposition-predicted ion distribution is quite similar to the one directly obtained from MD simulation of stepped electrodes: identical cation/anion peak/trough locations with similar magnitudes. The mechanism underlying this phenomenon can be explained by the structure interference theory: (1) the ion layer spacing near 0-step planar electrode is determined by ion size, which is ~0.7 nm[26]; (2) as for 1-step electrode, shifted by 0.341 nm in z direction, the peak and trough of ion distribution profiles are overlapped with the trough and peak of the unshifted one, respectively, resulting in weakened peak and trough; (3) for 2-step electrode, the ion peak and trough shifted by 0.682 nm in z direction are overlapped with those of unshifted one, respectively, therefore leading to enhanced ion peak and trough. This structure interference can also be applied to ion distribution at stepped electrode with charges. The ion distribution in EDL with the surface charge density of 0.1 C/m^2 is reported in Figure 4a for 0-step electrode; the ion distribution profiles at 1-step electrode surface, obtained directly from MD simulation and processed via the interference theory, are shown in Figure 4b. It can be observed that in order to neutralize the positive charges on electrode, more anions are concentrated at the location of the first peak; the oscillation behavior of hierarchical structure becomes stronger due to the electrical shielding[45]; similarly, the oscillation behavior becomes weaker at charged 1-step electrode compared with charged 0-step electrode.

To obtain more detailed information of interfacial microstructure of ILs, we analyzed the 2-D ion density in xz plane at 1-step graphite electrode. As shown in Figure 5, it is found that at neutral surface, the cation/anion layering is still a key

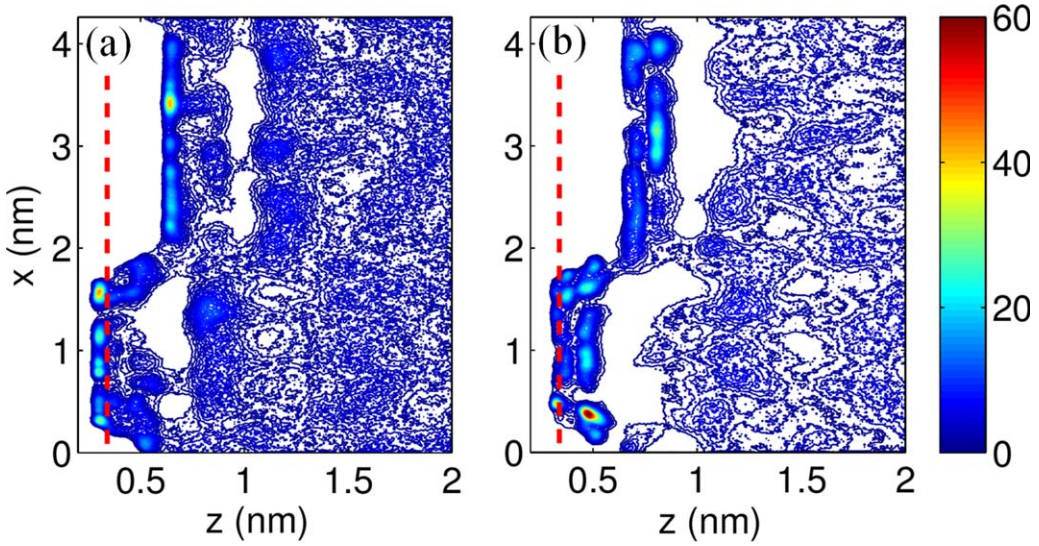

Figure 5. Two-dimensional number density distribution of cations (a) and anions (b) near neutral 1-step graphite electrode.

The red dashed line represents the position of the half-sized graphene. The unit of color bar is #/nm^3. [Color figure can be viewed in the online issue, which is available at wileyonlinelibrary.com.]

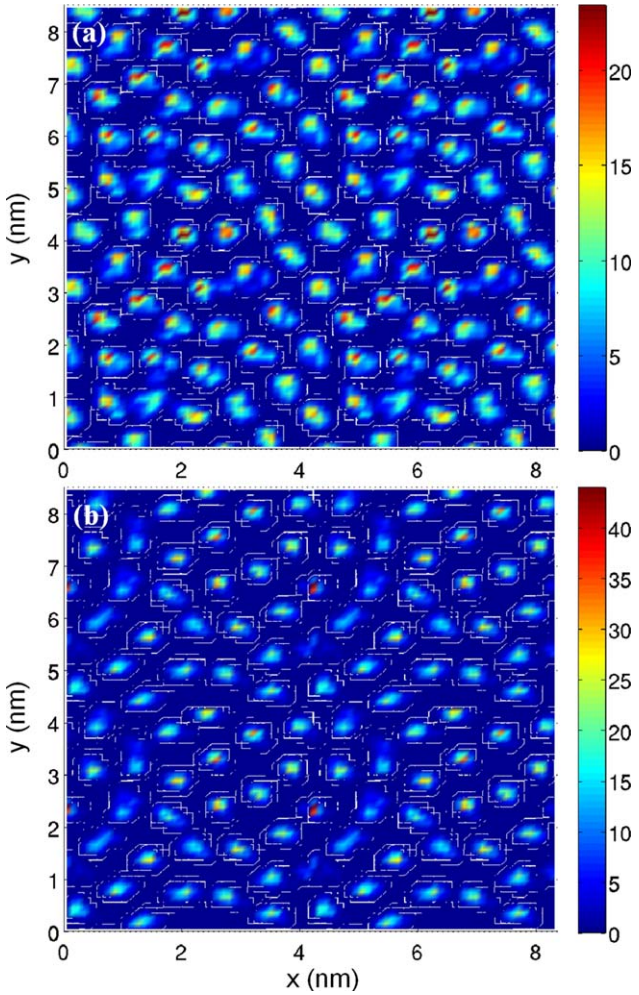

Figure 6. Two-dimensional number density distribution of cations (a) and anions (b) in the first ion layers near neutral 0-step graphite electrode.

The unit of color bar is #/nm^3. [Color figure can be viewed in the online issue, which is available at wileyonlinelibrary.com.]

feature for interfacial ILs.[18,29,30] Cations are closer to the surface than anions, as the imidazolium ring tends to be parallel to the graphene sheet[18,29–31] and the size of cation is smaller than the anion, in particular, along the dimension vertical to the ring.[26] The region of high ion (both cation and anion) density on the graphene step (i.e., $x > \sim 2.0$ nm) corresponds to that of low ion density below the step (i.e., $x < \sim 2.0$ nm), so that there is less layering present in 1-D ion density profiles (Figure 2) that are generally measured by AFM along the direction vertical to the electrode surface.[21,22] Meanwhile, the 2-D ion structure becomes more disordered (i.e., ion layering is less defined) in the region near the step edge (i.e., $x \sim 2.0$ nm); the ion density decreases as well, which is similar to the observation by Mendonça et al.[46] that the surface roughness could result in a decreased ion density.

The structure-interference-predicted results could provide insight into experimental measurements. For instance, in AFM experiments,[20–23,28,33] AFM tips may easily detect the first cation/anion layer in 1-step electrode and more layers in 2-step electrode, since beyond the first layer the cation/anion layering is not quite evident for ILs near 1-step electrode but strong near 2-step electrode. In addition, the application of EDL interference theory is expanded by the comparative analyses. It is verified in this work that EDL interference theory works not only for the interference of EDL stemming from opposite-facing walls in slit pore of porous electrode,[43,44] but also for the lateral interference stemming from the electrodes on the same side.

Considering the structural transitions of EDLs occurring between neutral and charged situations,[47,48] to further examine the microstructure of ILs near the graphite electrode, the ion distribution was analyzed in xy plane of the electrode surface. As shown in Figure 6, the 2-D distribution of ions in the first ion layer (0–0.55 nm) near neutral 0-step electrode surface reveals that both cations and anions adsorb on the electrode in a certain pattern (loosely with a gap of an integer multiple of the ion size). When cations and anions are plotted in one figure (Figure 7a), it is shown that they are packed alternatively in xy plane of the electrode surface (i.e., a 2-D lattice with counter-ion and co-ion interlocked with each other like in an ionic crystal[42]), and homogenously distributed in an aligned pattern. However, the pattern of ion packing is less defined in the second layer (0.55–1.1 nm) as shown in Figure 7b. This may be ascribed to the fact that the ions further from the electrode surface are less influenced by the solid surface confinement. The 2-D ion distribution changed obviously as the electrode surface was charged with a surface charge density of 0.1 C/m^2 in Figures 7c, d. Specifically, there are more anions than cations accumulated in the first layer, thus the counterion/co-ion lattice becomes obscure. But, there is still a certain pattern observed in this layer where anions dominate (i.e., the counterions are aligned). However, similar amounts of cations and anions in the second ion layer are observed, which are more randomly distributed compared with those in the first layer. In brief, at the charged electrode surface, the interlocked counterion/co-ion lattice of the first layer is less defined, whereas the ions of the second layer tend to be randomly distributed.

Conclusion and Prospective

The microscopic structure of ILs at different stepped electrode surfaces is studied by MD simulation in this work. Although the hierarchical structure and the alternative cation-anion distribution on stepped graphene are consistent with those reported for idealized graphene in literatures,[18,29–31] the stepped electrodes exhibit quantitatively distinctive ion distribution, which can be reasoned by the EDL interference theory. For 1-step electrode, the oscillation behavior is weakened due to the resultant deconstructive interference of the ion distribution functions from the idealized graphene and 1-stepped graphene, respectively, resulting in the homogenous ion distribution along z direction. For 2-step electrode, the oscillation is enhanced due to the constructive interference of the ion distribution functions from the idealized graphene and 2-stepped graphene, respectively, resulting in the heterogeneous ion distribution along z direction. As the step thickness (the vertical distance between the exposed half-sized graphene and the intact graphene) is approximately one half of (1-step) or identical to (2-step) the ion size, which determines the distance of two neighboring ion density peaks or troughs, the interference is either constructive or deconstructive depending on the coincidence of peak-trough or peak-peak (trough-trough). It should be noted that, for other ILs in which the ion size to the step thickness ratio is not nearly an integer, the ion distributions at stepped electrode may be more complicated, requiring further investigation. Furthermore, the 2-D number density

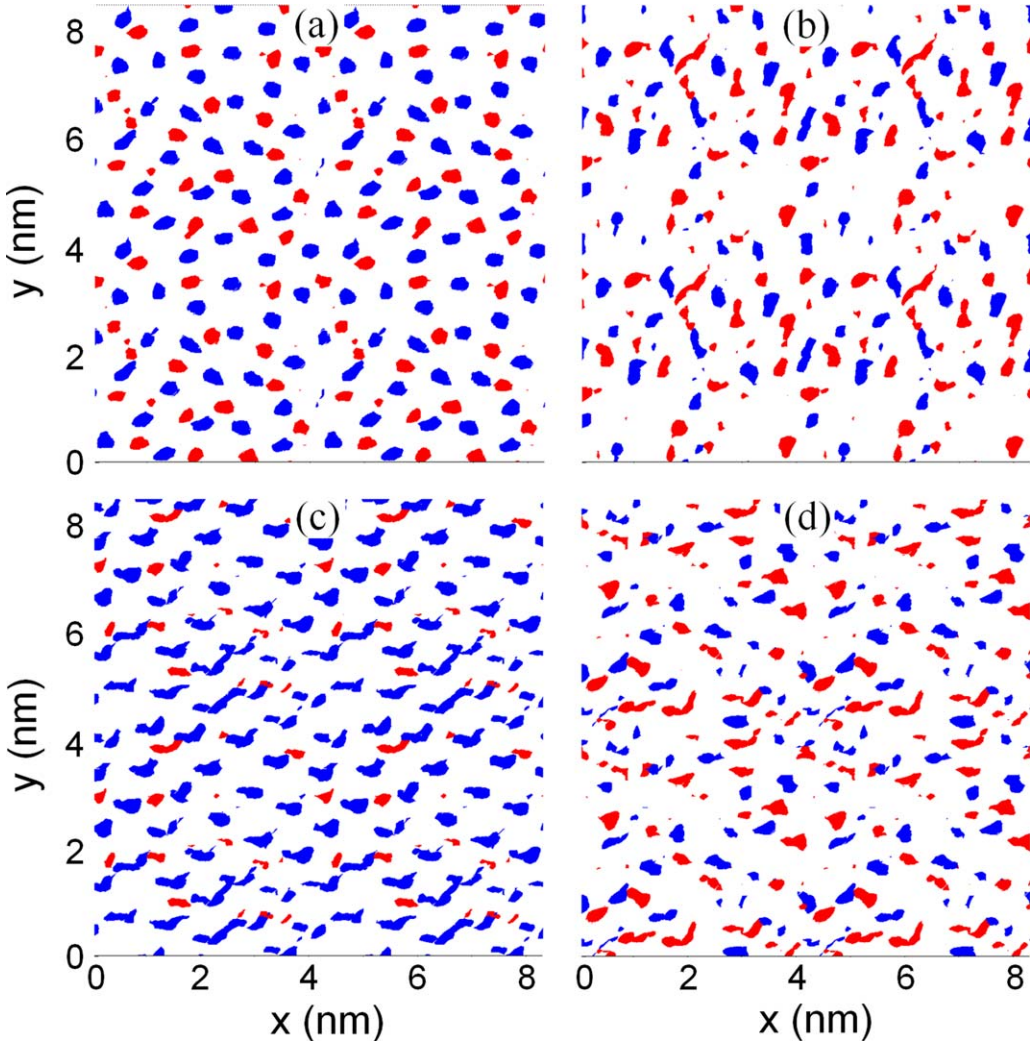

Figure 7. Two-dimensional number density distribution of cations (in red) and anions (in blue) in the first (a, c) and second (b, d) ion layers near 0-step graphite electrode with surface charge densities of 0 C/m^2 (a, b) and 0.1 C/m^2 (c, d).

Note the density larger than 6/nm^3 was shown. [Color figure can be viewed in the online issue, which is available at wileyonlinelibrary.com.]

distributions of cations and anions in the first and second layers near neutral 0-step graphite electrode were examined to exhibit different microstructures: at neutral electrodes, the ions are distributed as interlocked counterion/co-ion lattices in *xy* plane of electrode surface; at charged electrodes, the ions of the second ion layer are more randomly distributed than those of the first one.

It is worthy to note that although the carbon electrode used in this work is more complicated than the ideal nondefective electrode, the model of stepped structure is still a simplified one (e.g., step edge has a regular shape of zigzag or armchair) compared to the real electrode structure. Moreover, the changes in ion distribution stemming from stepped surface may impose a great impact on ion diffusion as well as the microscopic flow of electrolytes in supercapacitors.[42] Therefore, a great deal of effort is required to continue the study of the EDL microstructure and transport phenomena at more realistic surface (e.g., multistepped structure and irregular defect edge) in the future. In addition, there may be some functional groups decorated on the edge defect (e.g., hydroxyl, aldehyde, and carboxyl)[49,50] of carbon electrode generated by different synthesis methods. The role of these functional groups in ILs adsorption is still waiting for exploration.

Acknowledgments

G.F. and W.Z. acknowledge the support from Natural Science Foundation of Hubei Province of China (2014CFA089) and National Natural Science Foundation of China (51406060). P.T.C. acknowledges the support from the Fluid Interface Reactions, Structures and Transport (FIRST), an Energy Frontier Research Center funded by the U.S. Department of Energy, Office of Science, Office of Basic Energy Sciences. The work was partially carried out at National Supercomputer Center in Tianjin, and the calculations were performed on TianHe-1 (A). Computations were in part performed at the National Energy Research Scientific Computing Center, which is supported by the Office of Science of the U.S. Department of Energy under Contract DEAC02-05CH11231.

Literature Cited

1. Miller JR, Simon P. Materials science: electrochemical capacitors for energy management. *Science*. 2008;321(5889):651–652.
2. Christen T, Ohler C. Optimizing energy storage devices using Ragone plots. *J Power Sources*. 2002;110(1):107–116.
3. Burke A. R&D considerations for the performance and application of electrochemical capacitors. *Electrochim Acta*. 2007;53(3):1083–1091.
4. Simon P, Gogotsi Y. Materials for electrochemical capacitors. *Nat Mater*. 2008;7(11):845–854.
5. Conway BE. *Electrochemical Supercapacitors: Scientific Fundamentals and Technological Applications*. New York: Kluwer Academic, Plenum Publishers, 1999.
6. Gogotsi Y, Simon P. True performance metrics in electrochemical energy storage. *Science*. 2011;334(6058):917–918.
7. Zhang LL, Zhao X. Carbon-based materials as supercapacitor electrodes. *Chem Soc Rev*. 2009;38(9):2520–2531.
8. Simon P, Gogotsi Y. Capacitive energy storage in nanostructured carbon–electrolyte systems. *Acc Chem Res*. 2012;46(5):1094–1103.
9. Xu C, Xu B, Gu Y, Xiong Z, Sun J, Zhao X. Graphene-based electrodes for electrochemical energy storage. *Energy Environ Sci*. 2013; 6(5):1388–1414.
10. Ohno H. *Electrochemical Aspects of Ionic Liquids*. New York: Wiley-Interscience, 2005.
11. Kim TY, Lee HW, Stoller M, Dreyer DR, Bielawski CW, Ruoff RS, Suh KS. High-performance supercapacitors based on poly(ionic liquid)-modified graphene electrodes. *ACS Nano*. 2010;5(1):436–442.
12. Liu C, Yu Z, Neff D, Zhamu A, Jang BZ. Graphene-based supercapacitor with an ultrahigh energy density. *Nano Lett*. 2010;10(12): 4863–4868.
13. Zhou ZB, Matsumoto H, Tatsumi K. Low-melting, low-viscous, hydrophobic ionic liquids: aliphatic quaternary ammonium salts with perfluoroalkyltrifluoroborates. *Chem* Eur J. 2005;11(2):752–766.
14. Beguin F, Frackowiak E. *Supercapacitors*. Weinheim: Wiley-VCH, 2013.
15. Kondrat S, Kornyshev A. Superionic state in double-layer capacitors with nanoporous electrodes. *J Phys Condens Matter*. 2011;23(2): 022201.
16. Shim Y, Kim HJ. Nanoporous carbon supercapacitors in an ionic liquid: a computer simulation study. *ACS Nano*. 2010;4(4):2345–2355.
17. Feng G, Li S, Presser V, Cummings PT. Molecular insights into carbon supercapacitors based on room-temperature ionic liquids. *J Phys Chem Lett*. 2013;4(19):3367–3376.
18. Fedorov MV, Kornyshev AA. Ionic liquids at electrified interfaces. *Chem Rev*. 2014;114(5):2978–3036.
19. Mezger M, Schröder H, Reichert H, Schramm S, Okasinski JS, Schöder S, Honkimäki V, Deutsch M, Ocko BM, Ralston J. Molecular layering of fluorinated ionic liquids at a charged sapphire (0001) surface. *Science*. 2008;322(5900):424–428.
20. Atkin R, Borisenko N, Drüschler M, El Abedin SZ, Endres F, Hayes R, Huber B, Roling B. An in situ STM/AFM and impedance spectroscopy study of the extremely pure 1-butyl-1-methylpyrrolidinium tris (pentafluoroethyl) trifluorophosphate/Au (111) interface: potential dependent solvation layers and the herringbone reconstruction. *Phys Chem Chem Phys*. 2011;13(15):6849–6857.
21. Atkin R, Abedin SZE, Hayes R, Gasparotto LHS, Borisenko N, Endres F. AFM and STM studies on the surface interaction of [BMP]TFSA and [EMIm]TFSA ionic liquids with Au(111). *J Phys Chem C*. 2009;113(30):13266–13272.
22. Atkin R, Warr GG. Structure in confined room-temperature ionic liquids. *J Phys Chem C*. 2007;111(13):5162–5168.
23. Atkin R, Borisenko N, Drüschler M, Endres F, Hayes R, Huber B, Roling B. Structure and dynamics of the interfacial layer between ionic liquids and electrode materials. *J Mol Liq*. 2014;192:44–54.
24. Perkin S, Albrecht T, Klein J. Layering and shear properties of an ionic liquid, 1-ethyl-3-methylimidazolium ethylsulfate, confined to nano-films between mica surfaces. *Phys Chem Chem Phys*. 2010; 12(6):1243–1247.
25. Smith AM, Lovelock KR, Perkin S. Monolayer and bilayer structures in ionic liquids and their mixtures confined to nano-films. *Faraday Discuss*. 2013;167:279–292.
26. Perkin S, Crowhurst L, Niedermeyer H, Welton T, Smith AM, Gosvami NN. Self-assembly in the electrical double layer of ionic liquids. *Chem Commun*. 2011;47(23):6572–6574.
27. Perkin S. Ionic liquids in confined geometries. *Phys Chem Chem Phys*. 2012;14(15):5052–5062.
28. Smith AM, Lovelock KR, Gosvami NN, Licence P, Dolan A, Welton T, Perkin S. Monolayer to bilayer structural transition in confined pyrrolidinium-based ionic liquids. *J Phys Chem Lett*. 2013; 4(3):378–382.
29. Feng G, Zhang JS, Qiao R. Microstructure and capacitance of the electrical double layers at the interface of ionic liquids and planar electrodes. *J Phys Chem C*. 2009;113(11):4549–4559.
30. Vatamanu J, Borodin O, Smith GD. Molecular insights into the potential and temperature dependences of the differential capacitance of a room-temperature ionic liquid at graphite electrodes. *J Am Chem Soc*. 2010;132(42):14825–14833.
31. Sha M, Zhang F, Wu G, Fang H, Wang C, Chen S, Zhang Y, Hu J. Ordering layers of [bmim][PF_6] ionic liquid on graphite surfaces: molecular dynamics simulation. *J Chem Phys*. 2008;128(13):134504.
32. Wang S, Li S, Cao Z, Yan T. Molecular dynamic simulations of ionic liquids at graphite surface. *J Phys Chem C*. 2009;114(2):990–995.
33. Ivaništšev V, Fedorov M, Lynden-Bell R. Screening of ion–graphene electrode interactions by ionic liquids: the effects of liquid structure. *J Phys Chem C*. 2014;118(11):584–15847.
34. Black JM, Walters D, Labuda A, Feng G, Hillesheim PC, Dai S, Cummings PT, Kalinin SV, Proksch R, Balke N. Bias-dependent molecular-level structure of electrical double layer in ionic liquid on graphite. *Nano Lett*. 2013;13(12):5954–5960.
35. Zhou F, Liang Y, Liu W. Ionic liquid lubricants: designed chemistry for engineering applications. *Chem Soc Rev*. 2009;38(9):2590–2599.
36. Meunier V, Kalinin SV, Shin J, Baddorf AP, Harrison RJ. Quantitative analysis of electronic properties of carbon nanotubes by scanning probe microscopy: from atomic to mesoscopic length scales. *Phys Rev Lett*. 2004;93(24):246801.
37. Borodin O. Polarizable force field development and molecular dynamics simulations of ionic liquids. *J Phys Chem B*. 2009; 113(33):11463–11478.
38. Lindahl E, Hess B, van der Spoel D. GROMACS 3.0: a package for molecular simulation and trajectory analysis. *J Mol Model*. 2001; 7(8):306–317.
39. Yeh IC, Berkowitz ML. Ewald summation for systems with slab geometry. *J Chem Phys*. 1999;111(7):3155–3162.
40. Darden T, York D, Pedersen L. Particle mesh Ewald: an N•log(N) method for Ewald sums in large systems. *J Chem Phys*. 1993; 98(12):10089–10092.
41. Hess B, Bekker H, Berendsen HJ, Fraaije JG. LINCS: a linear constraint solver for molecular simulations. *J Comput Chem*. 1997; 18(12):1463–1472.
42. Kondrat S, Wu P, Qiao R, Kornyshev AA. Accelerating charging dynamics in subnanometre pores. *Nat Mater*. 2014;13(4):387–393.
43. Feng G, Cummings PT. Supercapacitor capacitance exhibits oscillatory behavior as a function of nanopore size. *J Phys Chem Lett*. 2011;2(22):2859–2864.
44. Jiang DE, Jin Z, Wu J. Oscillation of capacitance inside nanopores. *Nano Lett*. 2011;11(12):5373–5377.
45. Bazant MZ, Storey BD, Kornyshev AA. Double layer in ionic liquids: overscreening versus crowding. *Phys Rev Lett*. 2011;106(4): 046102.
46. Mendonça ACF, Pádua AAH, Malfreyt P. Nonequilibrium molecular simulations of new ionic lubricants at metallic surfaces: prediction of the friction. *J Chem Theory Comput*. 2013;9(3):1600–1610.
47. Merlet C, Limmer DT, Salanne M, van Roij R, Madden PA, Chandler D, Rotenberg B. The electric double layer has a life of its own. *J Phys Chem C*. 2014;118(32):18291–18298.
48. Kornyshev AA, Qiao R. Three-dimensional double layers. *J Phys Chem C*. 2014;118(32):18285–18290.
49. Shen J, Liu A, Tu Y, Foo G, Yeo C, Chan-Park MB, Jiang R, Chen Y. How carboxylic groups improve the performance of single-walled carbon nanotube electrochemical capacitors? *Energy Environ Sci*. 2011;4(10):4220–4229.
50. Wang M, Lai ZB, Galpaya D, Yan C, Hu N, Zhou L. Atomistic simulation of surface functionalization on the interfacial properties of graphene-polymer nanocomposites. *J Appl Phys*. 2014;115(12): 123520.

Manuscript received Apr. 1, 2015, and revision received May 23, 2015.